

A novel method for predicting and mapping the occurrence of sun glare using Google Street View



Xiaojiang Li^{a,*}, Bill Yang Cai^a, Waishan Qiu^a, Jinhua Zhao^b, Carlo Ratti^a

^a MIT Senseable City Lab, Department of Urban Studies and Planning, Massachusetts Institute of Technology, Room 9-250, 77 Massachusetts Avenue, Cambridge, MA 02139, United States

^b Department of Urban Studies and Planning, Massachusetts Institute of Technology, Cambridge, MA 02139, United States

ARTICLE INFO

Keywords:

Sun glare
Google Street View
Deep learning

ABSTRACT

The sun glare is one of the major environmental hazards that cause traffic accidents. Every year many traffic accidents are caused by sun glare in the United States. Providing accurate information about when and where sun glare happens would be helpful to prevent sun glare caused traffic accidents. In this study, we proposed to use the publicly accessible Google Street View (GSV) panorama images to estimate and predict the occurrence of sun glare. GSV images have view sight similar to drivers, which make GSV images suitable for estimating the visibility of sun glare to drivers. A recently developed convolutional neural network algorithm was used to segment GSV images and predict obstructions on sun glare. Based on the predicted obstructions for given locations, we further estimated the time windows of sun glare by calculating the sun positions and the relative angles between drivers and the sun for those locations. We conducted a case study in Cambridge, Massachusetts, USA. Results show that the method can predict the occurrence of sun glare precisely. The proposed method provides an important tool for people to deal with the sun glare and reduce the potential traffic accidents caused by the sun glare.

1. Introduction

The sun glare is one of the major safety hazards that cause traffic accident for drivers (Hagita and Mori, 2014; Jurado-Piña et al., 2010). When the sun is low during rising and setting and the sunlight may enter the field of view of drivers at some time with the right azimuth angles. The glare caused by sun would impair driver's vision and cause temporary blindness to drivers, both of which are annoying and dangerous for drivers (Aune, 2017). Hagita and Mori (2014) investigated the effects of sun glare on traffic accidents. Results show that the presence of sun glare is connected with traffic accidents of cars and cyclists. Hagita and Mori (2013) examined the associations between sun glare and bicycle and pedestrian accidents in Chiba prefecture, Japan. Results show that sun glare increases traffic accidents in cases of oncoming bicycles and pedestrians encountering turning vehicles significantly. In addition, the presence of sun glare would also slow down traffic flows and cause traffic congestions (Auffray, 2007; Churchill et al., 2012).

Visor and tinting are very commonly used method to deal with sun glare. However, the visor would obstruct driver's overall vision, while driving without obstruction is one of the basic requirements for safe driving. In addition, the visor and the tinting only cover a small portion of the front windshield and cannot screen out the sun (Hagita and Mori, 2013). The visor also blocks driver's view sight to see the overhead traffic light. Knowing when and where the sun glare occurs would get drivers be prepared (i.e. change route or schedule) and alerted to avoid the potential sun glare caused traffic accidents and congestions. For road builders, knowing

* Corresponding author.

E-mail address: lixiaojiang.gis@gmail.com (X. Li).

the spatio-temporal distributions of sun glare would be helpful to design safer road networks. Accurate prediction of the occurrence of the sun glare is thus needed.

The occurrence of sun glares is determined by the sun's angle in relation to drivers, which is further influenced by the sun elevation, azimuth, driving direction, and slope angle. The terrain changes and obstructions along roads could block the sunlight from shining to driver's eyes. Currently, using the digital terrain model and the road network map is the most widely used method to predict the occurrence of the sun glare (Hagita and Mori, 2014; Aune, 2017). The sun position at a specific time of the vehicle's relative location can be precisely estimated. Based on the geometrical model between the driver and the sun position, the occurrence of the sun glare can be predicted (Jurado-Piña et al., 2010). While the digital terrain model considers of the obstruction effect of sun glare caused by the terrain, however, the obstructions of the building blocks and trees on both sides of roads are not considered in the digital terrain based method. In addition, the high spatial resolution digital terrain model is usually required for accurate sun glare prediction. However, high spatial resolution digital terrain models usually are not available.

In this study, we proposed to use the Google Street View (GSV) panorama images to predict the occurrence of sun glare. Since GSV images were taken by moving vehicles on the road (Li et al., 2015), those street-level images perfectly represent driver's visual experience in driving. In addition, GSV images capture the obstructions along roads at a fine level, which would further provide accurate information of obstructions along roads. We used the state-of-the-art deep convolutional neural network algorithm to segment GSV images and classify those obstruction pixels from GSV images. Based on the image segmentation results and the geometrical model of the sun and drivers, we predicted the occurrence of sun glare with consideration of all obstructions such as, terrain changes, trees, buildings, etc. This study provides a very cheap and efficient way to predict the spatio-temporal distribution of the sun glare at a large scale precisely.

2. Methodology

2.1. Study area and dataset preparation

City of Cambridge, Massachusetts was selected as the case study area. In order to create sample sites in the study area, we first split each street segment by the distance of 40 m. The cutting points of those street segments were used as the sample sites to collect Google Street View (GSV) panorama images and visualize the sun glare occurrence. Fig. 1(a) shows the generated sample sites along streets of Cambridge, Massachusetts. Based on the coordinates of those created sample sites, we further collected metadata of GSV panoramas (Fig. 1(b)) using Google Street View metadata application programming interface (API) (Li et al., 2018). The following user resource locator (URL) is an example of accessing the metadata of GSV panorama using the coordinate as input.

```
https://maps.googleapis.com/maps/api/streetview/metadata?size=400x400&location=42.400666,-71.138646&heading=HEADING&fov=60&pitch=0&key=API\_KEY
```

Metadata of a GSV panorama

```
GSV metadata json file
{
  "copyright": "© 2019 Google",
  "date": "2014-09",
  "location": {
    "lat": 42.399666,
    "lng": -71.138656
  },
  "yaw": 264.010559
  "tilt": 0.53
  "pano_id": "zJ7VBv6pFixr7nY8U2fJbQ",
  "status": "OK"
}
```

In the above URL example, users also need to register on Google Maps Platform (<https://developers.google.com/maps/documentation/>) and provide billing information in order to have a valid API key. The collected metadata includes the acquisition date, panorama ID, coordinate of the panorama, yaw angle, and tilt angle. Based on the panorama IDs of the created sample sites in the study area, we further collected the GSV panoramas using Google Map Application Programming Interface (APIs) from Google Server (Fig. 1(c)). In this study, we developed a Python script to download GSV panoramas for all sites using the coordinates of those sample sites as the input.

2.2. Google Street View (GSV) panoramas segmentation

Recent progresses in artificial intelligence make it possible to recognize obstructions along streets from GSV panoramas accurately. In this study, we used the Pyramid Scene Parsing Network (PSPNet), which is a deep convolutional neural network trained on the ADE20K dataset (Zhao et al., 2017; Zhou et al., 2017), to segment GSV panoramas. The PSPNet has achieved the state-of-the-art performance in pixel-level segmentation of complex visual scenes with overall accuracy higher than 80%. Hence, the validated performance of the PSPNet gives us confidence in our use of the PSPNet to accurately classify GSV panoramas into sky, buildings, trees, ground, and other environmental factors. Fig. 2 shows the image segmentation results on GSV panoramas using the PSPNet.

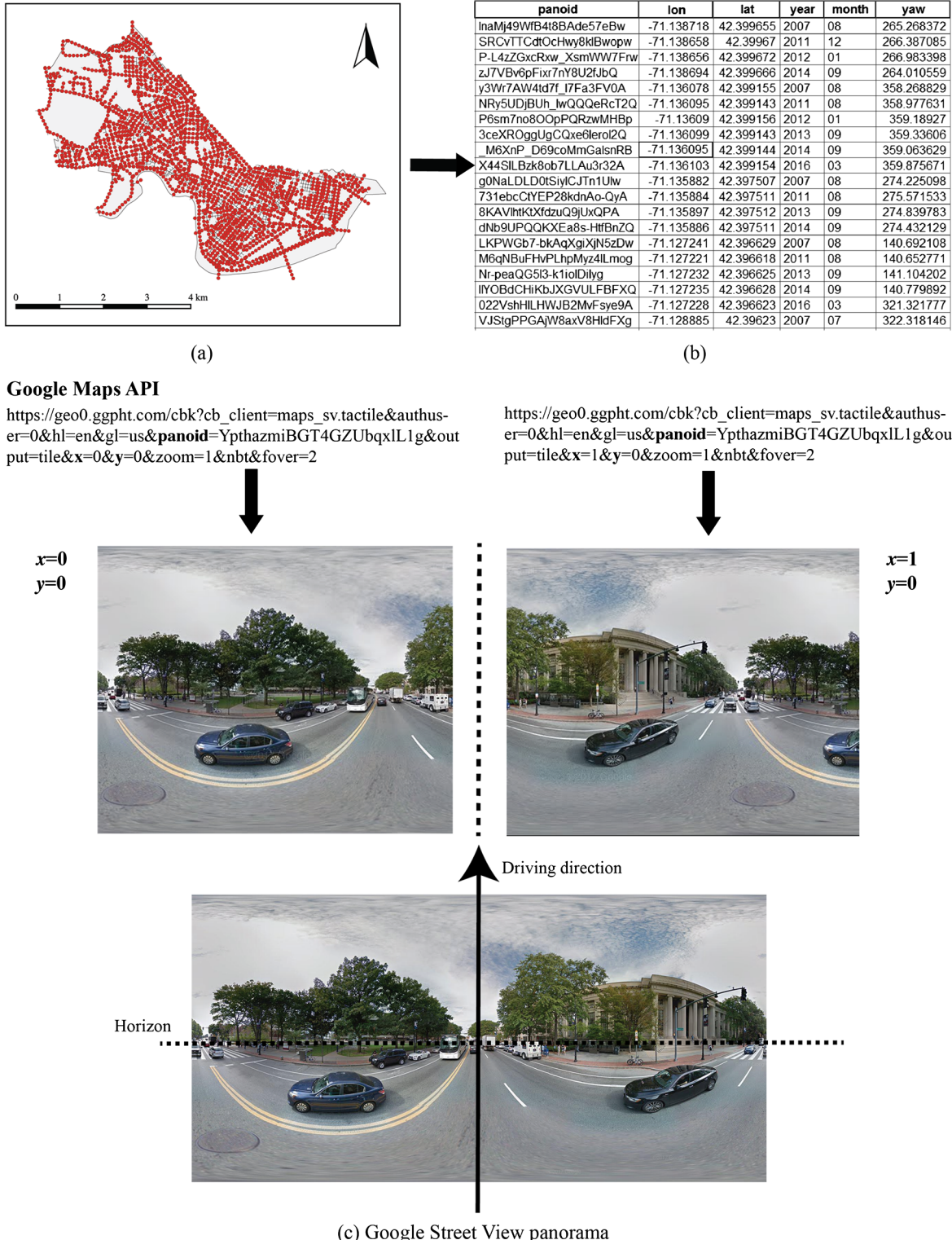


Fig. 1. The workflow for GSV panorama collection in Cambridge, (a) the created sample sites (b) the metadata of GSV panoramas, (c) a collected GSV panorama of one sample site using Google Map API.

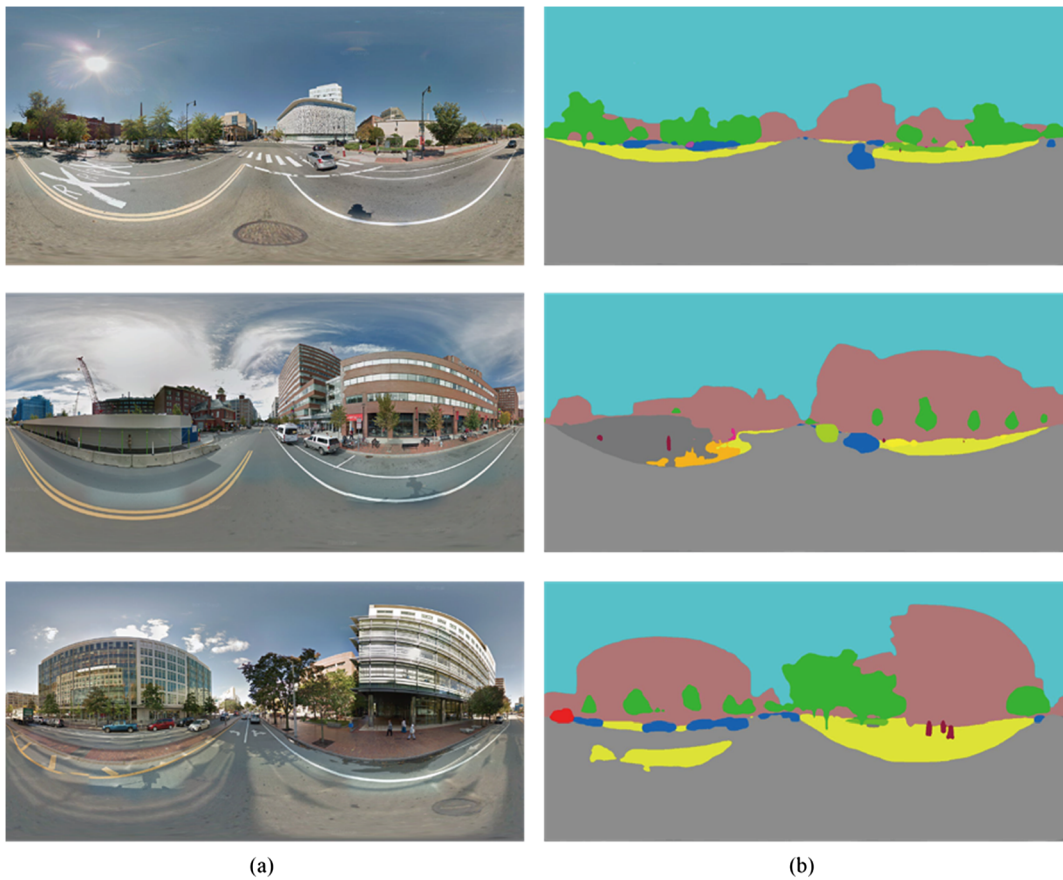


Fig. 2. Image segmentation results on GSV panoramas using pyramid scene parsing convolutional neural network (PSPNet).

Those non-sky pixels were considered as obstructions, which would block the glaring sun.

2.3. Sun glare prediction

Estimation of the sun position is prerequisite for sun glare prediction. The sun position of one location (lon , lat) at a specific time can be represented by sun elevation θ and azimuth angle ϕ (anticlockwise from east) (Fig. 3(a)). The sun elevation θ and clockwise azimuth angle ϕ' (clockwise from north) can be calculated as (Reda and Andreas, 2004; NOAA, 2014),

$$\cos(90 - \theta) = \sin(lat)\sin(\delta) + \cos(lat)\cos(\delta)\cos(ha) \quad (1)$$

$$\cos(180 - \phi') = -\frac{\sin(lat)\cos(90 - \theta) - \sin(ha)}{\cos(lat)\sin(90 - \theta)} \quad (2)$$

$$\phi = 90 - \phi', \quad \text{if } \phi < 0; \phi = \phi + 360 \quad (3)$$

where lon , lat are the longitude and latitude of location, δ is the solar declination, ha is the hour angle.

The solar declination δ can be calculated as,

$$\delta = 0.006918 - 0.399912\cos(\gamma) + 0.070257\sin(\gamma) - 0.006758\cos(2\gamma) + 0.000907\sin(2\gamma) - 0.002697\cos(3\gamma) + 0.00148\sin(3\gamma) \quad (4)$$

The γ is the fractional year and can be calculated as,

$$\gamma = \frac{2\pi}{Y} \left(d - 1 + \frac{hr - 12}{24} \right), \quad Y = 365 \quad (5)$$

where d is the day of year, hr is the hour in one day, Y is 366 for leap year.

The solar hour angle ha can be calculated as:

$$ha = tst/4 - 180 \quad (6)$$

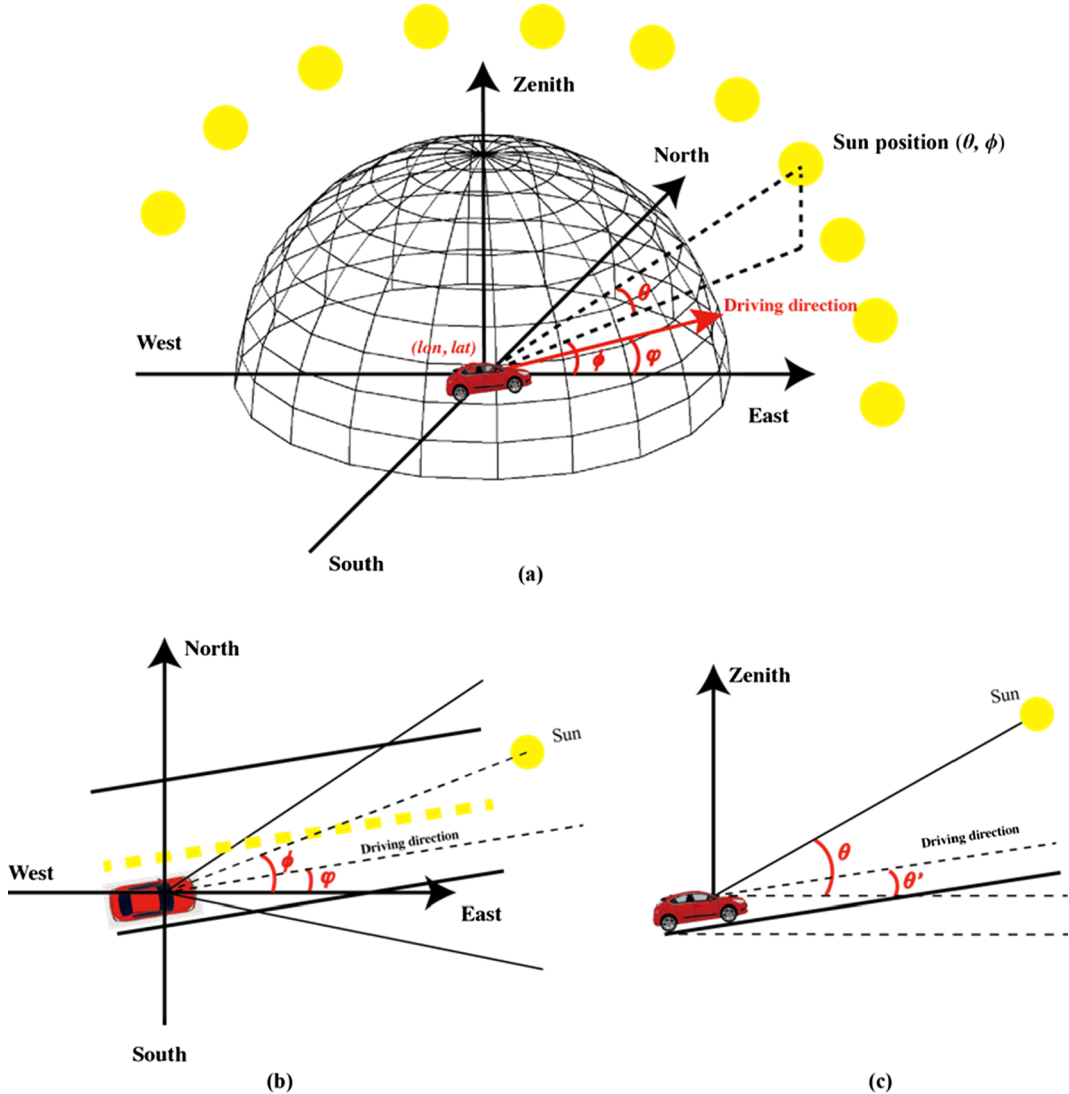


Fig. 3. The geometrical model of the sun position and the location of vehicle on driveway.

$$tst = hr * 60 + mn + sc/60 + time_{offset} \quad (7)$$

$$time_{offset} = et + 4 * lon - 60 * timezone \quad (8)$$

where

mn is the minute (0–59),
 sc is the second (0–59),

$$et = 229.18 * (0.000075 + 0.001868\cos(\gamma) - 0.032077\sin(\gamma) - 0.014615\cos(2\gamma) - 0.040849\sin(2\gamma)) \quad (9)$$

lon is the longitude of the location,
 $timezone$ is in hours from UTC.

In this study, we used an open source python module “*pysolar*” to estimate the sun position for the samples sites in the study area at any specific time. Since the latitude of the study area is not greater than 72° north, therefore, the effects of atmospheric reflection is not considered (NOAA Solar Position Calculator, <https://www.esrl.noaa.gov/gmd/grad/solcalc/azel.html>).

Fig. 3(a) shows the geometrical model of the sun position and the location of a car driving through point (lon, lat) , therefore, the relative horizontal direction between sun and the car is (Fig. 3(b)),

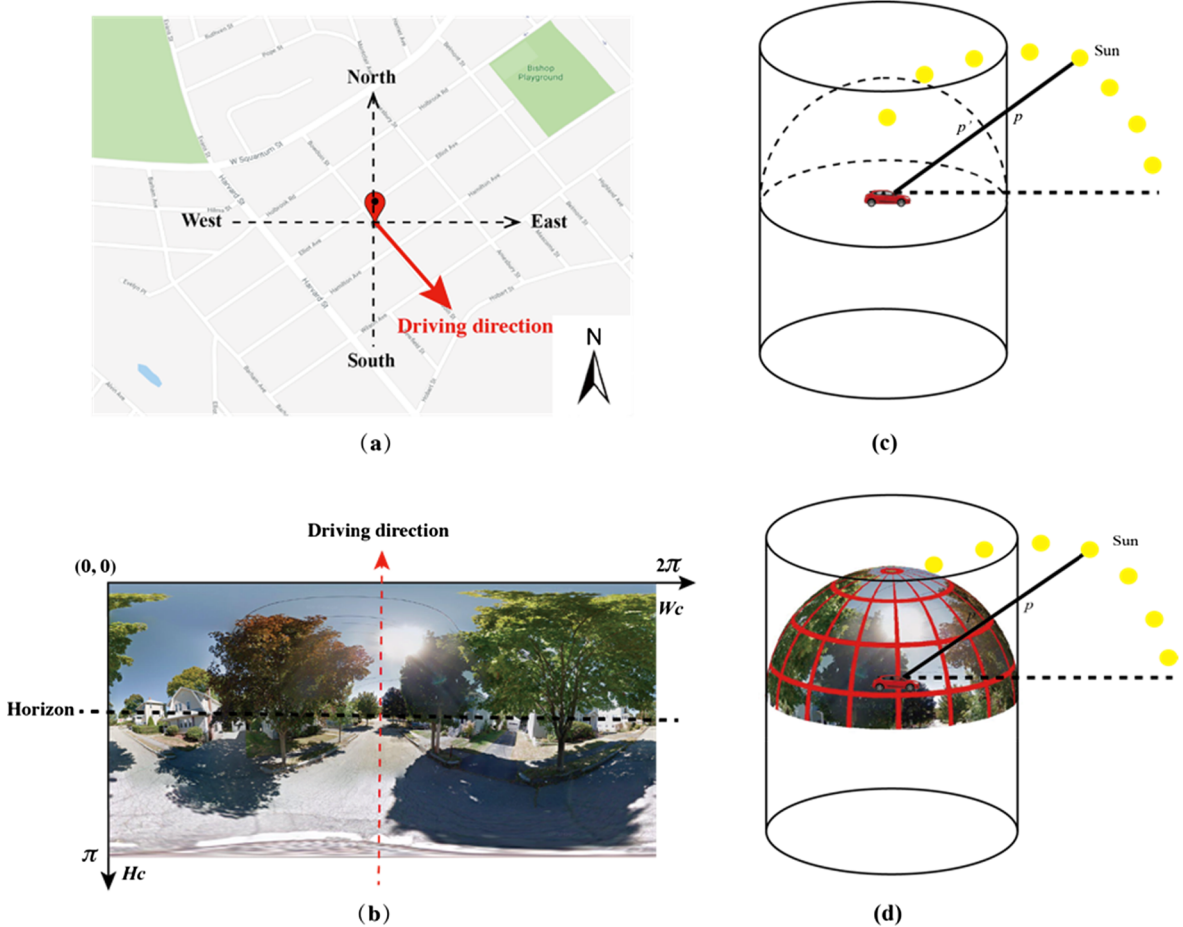


Fig. 4. The geometrical model of projecting sun position at a certain time on a cylindrical GSV panorama.

$$h_glare = |\phi - \varphi| \quad (10)$$

where φ is the driving direction (anticlockwise from east). The relative vertical angle of the car and sun is (Fig. 3(c)),

$$v_glare = |\theta - \theta'| \quad (11)$$

where θ' is the slope angle of the driveway. The driving direction φ and the slope angle θ' of the driveway are the yaw angle and tilt angle respectively, which both can be accessed from the GSV metadata (section 2.1). Based on previous studies (Jurado-Piña and Mayora, 2009b; Aune, 2017), if the h_glare and v_glare both are lower than 25° and there is no obstruction of the sun light, sun would cause glare.

The existence of the obstructions on sides of the driveways could block the sun glare. In this study, GSV panoramas were used to judge if the sun glare is obstructed or not based on the segmented GSV panoramas. Fig. 4 shows the geometrical model of projecting sun positions on GSV panoramas. The incidence point located on the cylindrical GSV panorama should be (x_c, y_c) ,

$$x_c = \frac{\varphi - \phi}{2\pi} W_c + C_x \quad (12)$$

$$y_c = C_y - \frac{\theta - \theta'}{\pi/2} H_c \quad (13)$$

where W_c is the width of the cylindrical GSV panorama, H_c is the height of the cylindrical GSV panorama, and the (C_x, C_y) is the central pixel of the GSV panorama,

$$\begin{aligned} C_x &= \frac{W_c}{2} \\ C_y &= \frac{H_c}{2} \end{aligned} \quad (14)$$

Whether the sun is obstructed or not can be estimated by judging whether the incidence point on the GSV panorama is open sky pixel or non-sky obstruction pixel. If the incidence point on the GSV panorama is non-sky pixel, therefore, the sun is obstructed, and the driver at this time of this location has no sun glare.

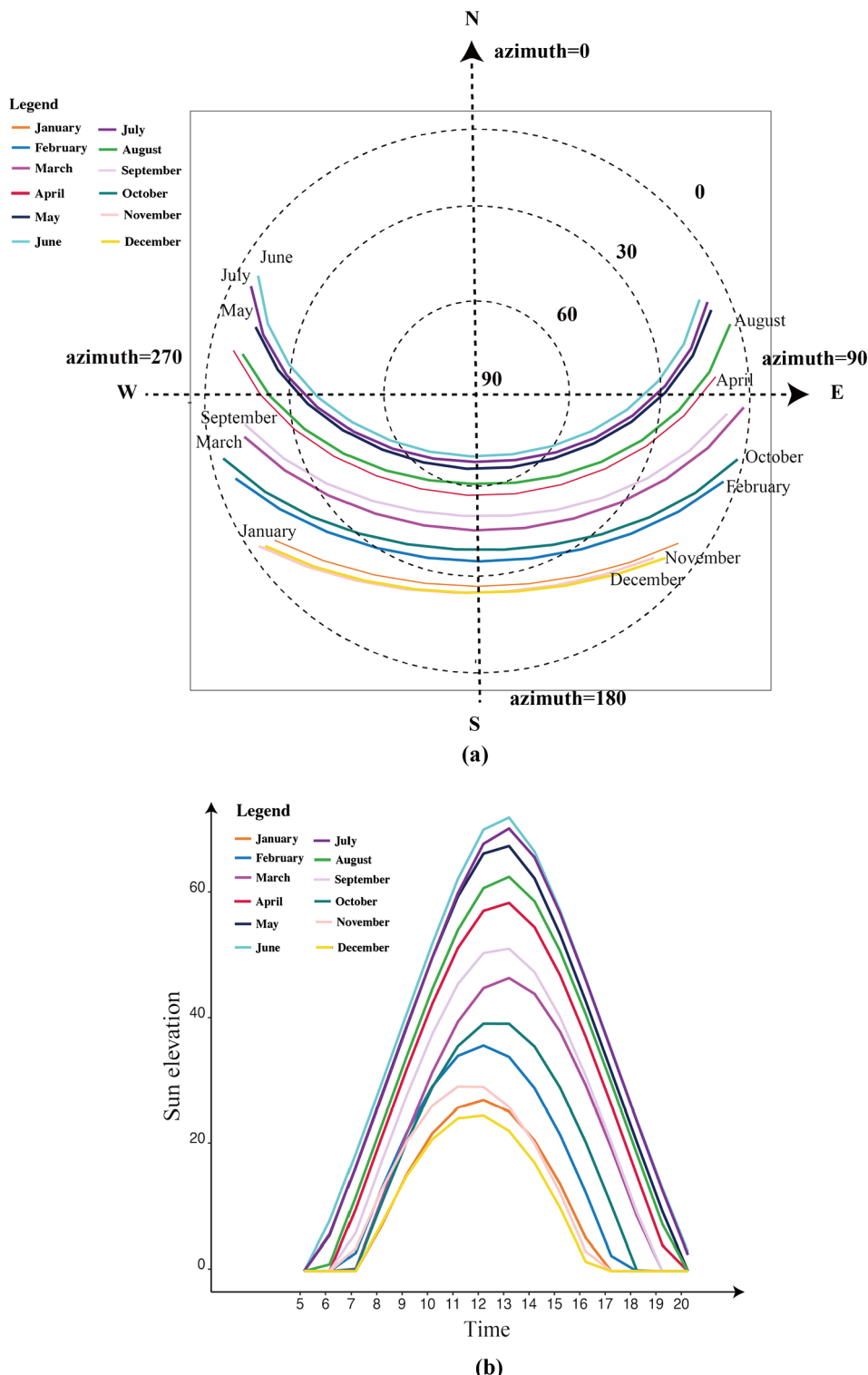


Fig. 5. The sun elevation and sun azimuth angles from 5 am to 8 pm on 20th day of different months in Cambridge, MA, (a) the sun diagram of Cambridge in one year, (b) the profiles of the sun elevation angles from 5 am to 8 pm on 20th day of different months.

Table 1

The ranges of street orientations with sunrise and sunset sun glare at Cambridge, MA (42.376, −71.117) based on the 25-degree criteria.

Date, 2018	Sunrise sun glare (time, ranges)	Sunset sun glare (time, ranges)
January 20th	8 am, [100.87, 150.87]	2 pm, [186.47, 236.47]
	9 am, [112.51, 162.51]	3 pm, [199.44, 249.44]
	10 am, [125.72, 175.72]	4 pm, [210.87, 260.87]
February 20th	7 am, [83.46, 133.46]	3 pm, [204.39, 254.39]
	8 am, [94.29, 144.29]	4 pm, [216.58, 266.58]
	9 am, [106.58, 156.58]	5 pm, [227.36, 277.36]
March 20th	8 am, [76.74, 126.74]	5 pm, [225.43, 275.43]
	9 am, [87.93, 137.93]	6 pm, [236.31, 286.31]
	7 am, [59.16, 109.16]	6 pm, [246.62, 296.62]
April 20th	8 am, [69.24, 119.24]	7 pm, [256.53, 306.53]
	6 am, [43.47, 93.47]	6 pm, [253.74, 303.74]
	7 am, [52.95, 102.95]	7 pm, [263.17, 313.17]
May 20th	6 am, [40.15, 90.15]	6 pm, [255.77, 305.77]
	7 am, [49.40, 99.40]	7 pm, [264.92, 314.92]
	6 am, [41.43, 91.43]	8 pm, [274.40, 324.40]
July 20th	7 am, [50.93, 100.93]	6 pm, [252.54, 302.54]
	7 am, [57.82, 107.82]	7 pm, [261.93, 311.93]
	8 am, [67.84, 117.84]	6 pm, [246.25, 296.25]
September 20th	7 am, [68.01, 118.01]	7 pm, [256.14, 306.14]
	8 am, [78.45, 128.45]	5 pm, [228.65, 278.65]
	8 am, [88.26, 138.26]	6 pm, [239.27, 289.27]
October, 20th	9 am, [99.75 149.75]	4 pm, [210.60, 260.60]
	7 am, [94.54, 144.54]	5 pm, [222.02, 272.02]
	8 am, [105.44, 155.44]	1 pm, [178.34, 228.34]
November 20th	9 am, [117.76, 167.76]	2 pm, [192.28, 242.28]
	10 am, [131.72, 181.32]	3 pm, [204.57, 254.57]
	8 am, [105.45, 155.45]	4 pm, [215.45, 265.45]
December 20th	9 am, [117.08, 167.08]	12 pm, [159.55, 209.55]
	10 am, [130.15, 180.15]	1 pm, [174.28, 224.28]
	11 am, [144.52, 194.52]	2 pm, [187.92, 237.92]
		3 pm, [200.11, 250.11]

3. Results

The sun glare usually happens during sun rising and sun setting when the sun is very low in the sky. Fig. 5 shows the profiles of sun elevation and azimuth angles from 5 am to 8 pm on 20th days of different months in one year at Cambridge, Massachusetts. In Cambridge, June has the highest sun in one year, and December has the lowest sun in one year (Fig. 5(a)–(b)).

If obstructions are not considered, sun glare happens when the relative horizontal direction and the relative vertical angle between sun and the car both are less than 25° (Fig. 3(b), (c)). The occurrence of sun glare is influenced by the locations and the orientations of streets. In the study area of Massachusetts, those streets in the direction of the southeast and southwest have larger possibility to have sun glare in one day. In summer, those streets toward the northeast and northwest will also have the possibility of having sun glare at morning and afternoon, respectively. In winter, the sun position is more southward, and the streets on the direction of the northeast and northwest have no sunrise and sunset sun glare. Table 1 presents the time at hour level and ranges of the street orientations for sun glare occurrence for 20th day in different months of 2018 if the obstruction along streets is not considered. Under no obstruction situation, the street orientation ranges for sun glare occurrence shift in different months of one year. Generally, in winter (e.g. December 20th, January 20th), driving toward northeast and northwest will have no risk of meeting sun glare in one day. The sunrise sun glare and sunset sun glare happen while driving toward southeast and southwest, respectively. In summer (e.g. June 20th, July 20th), because sun is highest in one year, driving toward northeast and northwest will have the sunrise and sunset sun glare, respectively.

Based on the ranges of street orientation (Table 1), those streets have sunrise glare and sunset glare on Dec 20th have orientations in range of 105–195° and 159–251°, respectively. This can be further confirmed by the spatial patterns of the sunrise sun glare (Fig. 6(a)) and sunset sun glare (Fig. 6(b)) on Dec 20th. Those streets orient to southeast have sunrise sun glare, those streets orient southwest have sunset sun glare. On June 20th, streets with orientation in ranges of 40–60° and 255–324° have sunrise and sunset sun glares, respectively. Fig. 6(c), (d) shows the spatial distributions of the sunrise and sunset glares on June 20th, respectively. Those streets orient to southeast have sunrise sun glare, those streets orient southwest have sunset sun glare.

The actual occurrence of the sun glare map is not only influenced by the orientation of the streets, but also the existence of obstructions between the driving car and the solar position. In order to map the actual sun glare map, we collected all historical Google Street View (GSV) panoramas with time stamps for all sample sites in the study area. We categorized all GSV panoramas by time stamp into leaf-on season (May, June, July, August, September, and October) and leaf-off season (November, December, January, February, March, and April). Fig. 7(a), (b) show the spatial distributions of available GSV panoramas that were captured in

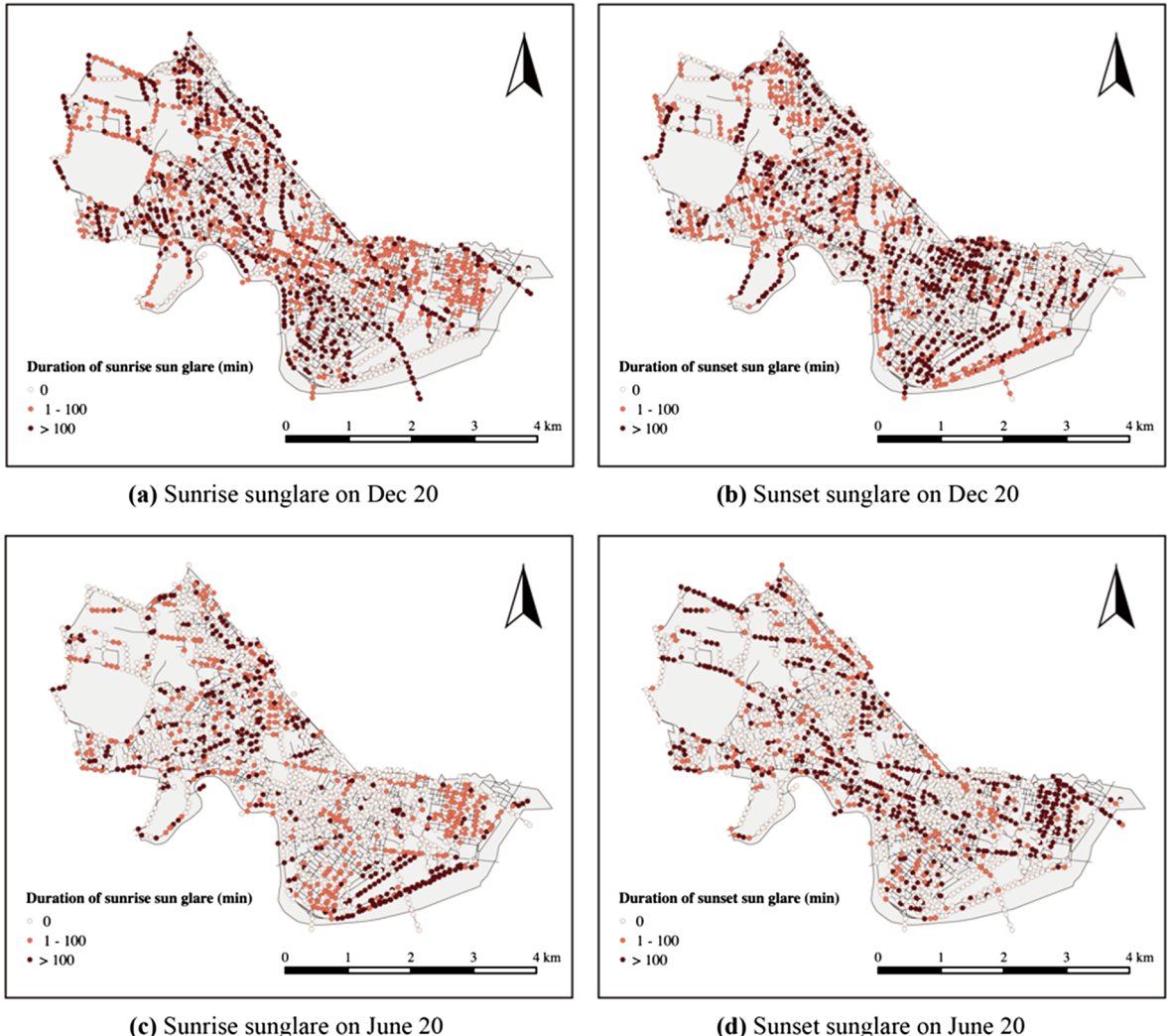


Fig. 6. The spatial distributions of the sunrise and sunset sun glares without considering the obstruction on sides of roads, (a) the spatial distribution of sunrise sun glare on December 20th, (b) the spatial distribution of the sunset sun glare on December 20th, (c) the spatial distribution of sunrise sun glare on June 20th, (d) the spatial distribution of sunset sun glare on June 20th.

leaf-on season and leaf-off season, respectively. Based on these spatial distributions, we found that most sample sites have summer-captured GSV panoramas available (Fig. 7(a)). However, there are only 400 sites having GSV panoramas captured in winter (Fig. 7(b)). These 400 sites are not suitable to map the whole spatial distribution of the sun glare in winter in the study area. Therefore, it is not suitable to generate sun glare maps for winter based on GSV images currently in the study area. With more street-level images available in winter in future, it would be possible to map the spatio-temporal distributions of the sun glare map. In this study, we only present the sun glare map in leaf-on season.

Based on the sun elevation and the azimuth, the sun path can be projected to the cylindrical GSV panorama. Fig. 8 shows the sun paths at different hours in days of July 15th, August 15th, September 15th, and October 15th in 2018. We assumed the existence of the buildings and trees would block the sun glare. Therefore, sun glare would be obstructed if sun position were not on sky pixels.

In order to validate the proposed GSV panorama-based method on predicting the obstruction of sunlight, we further took *in situ* measurement in the study area. Fig. 9 shows the comparison of the predicted sun path of July 5th on a GSV panorama (Fig. 9(a), (c)) and actual sun positions on photos taken at the same location (Fig. 9(b)). The predicted result shows that the sun is obstructed at 6:45 pm and the photos taken in fieldwork show that the sun is obstructed at 6:46 pm. We further compared the predicted sun paths and the actual sun positions at 7 other locations. The validation results show that the proposed method can estimate the exact time point of sun glare been blocked with an error of less than 3 min, which further prove that the proposed method based on GSV panoramas can estimate the obstruction of sunlight with high accuracy.

Fig. 10 shows the spatial distributions of the sun glare in the study area on June 20th and September 20th with consideration of obstructions along the streets. Compared with the sun glare maps without considering the obstruction (Fig. 6), the existence of

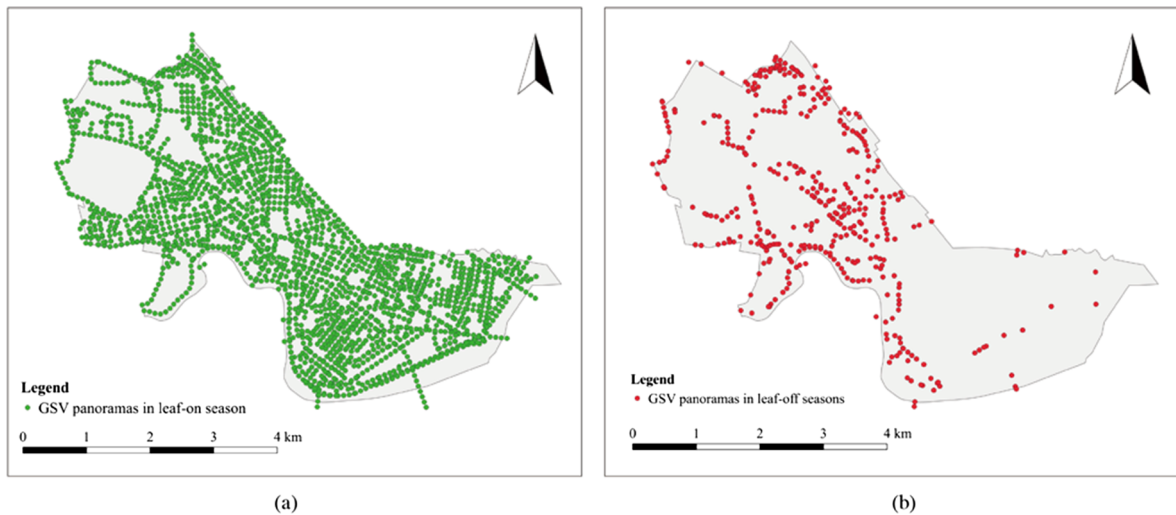


Fig. 7. The spatial distributions of available GSV panoramas in leaf-on season (a) and leaf-off season (b).

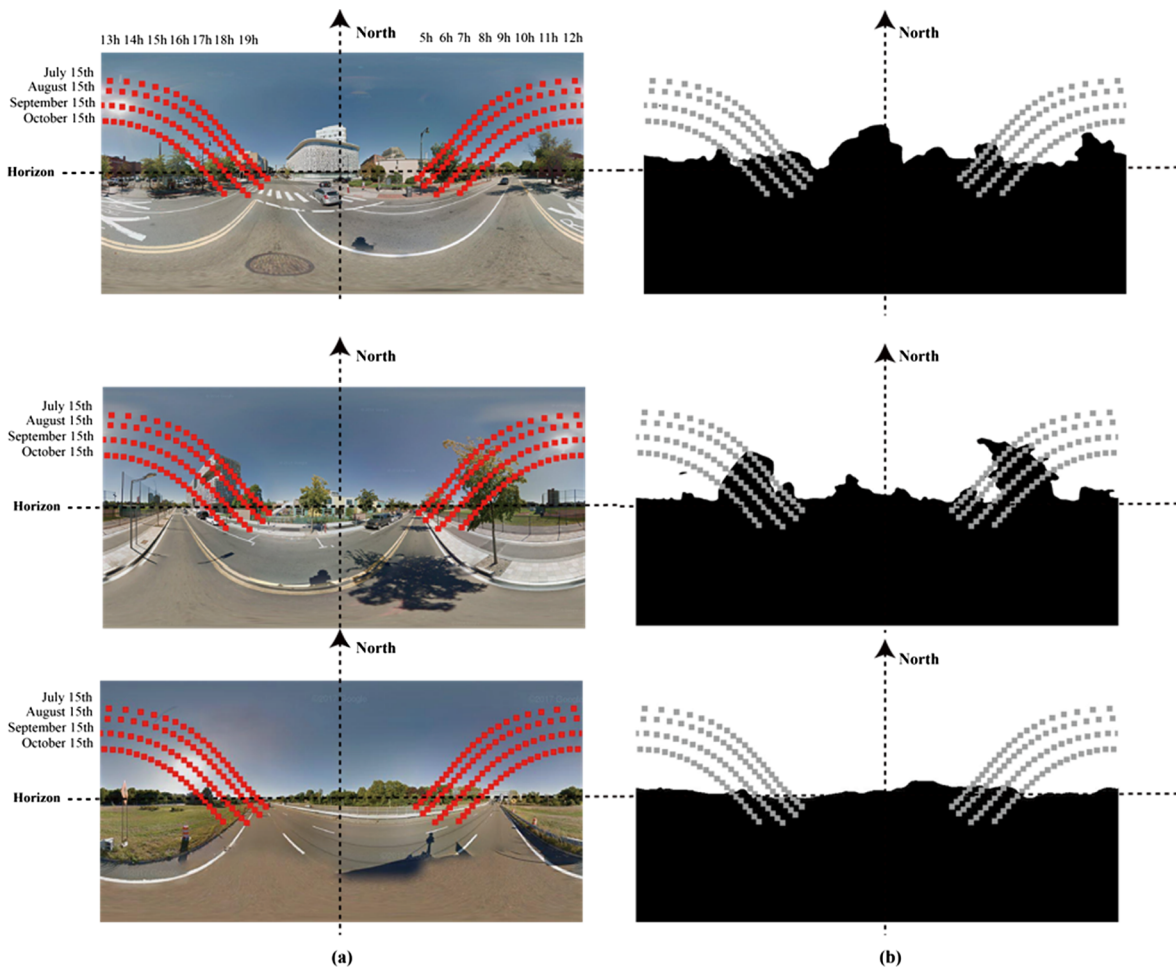


Fig. 8. The sun paths in July 15th, August 15th, September 15th, and October 15th on cylindrical Google Street View panoramas (a) and the segmented cylindrical panoramas (b) at three sites of the study area.

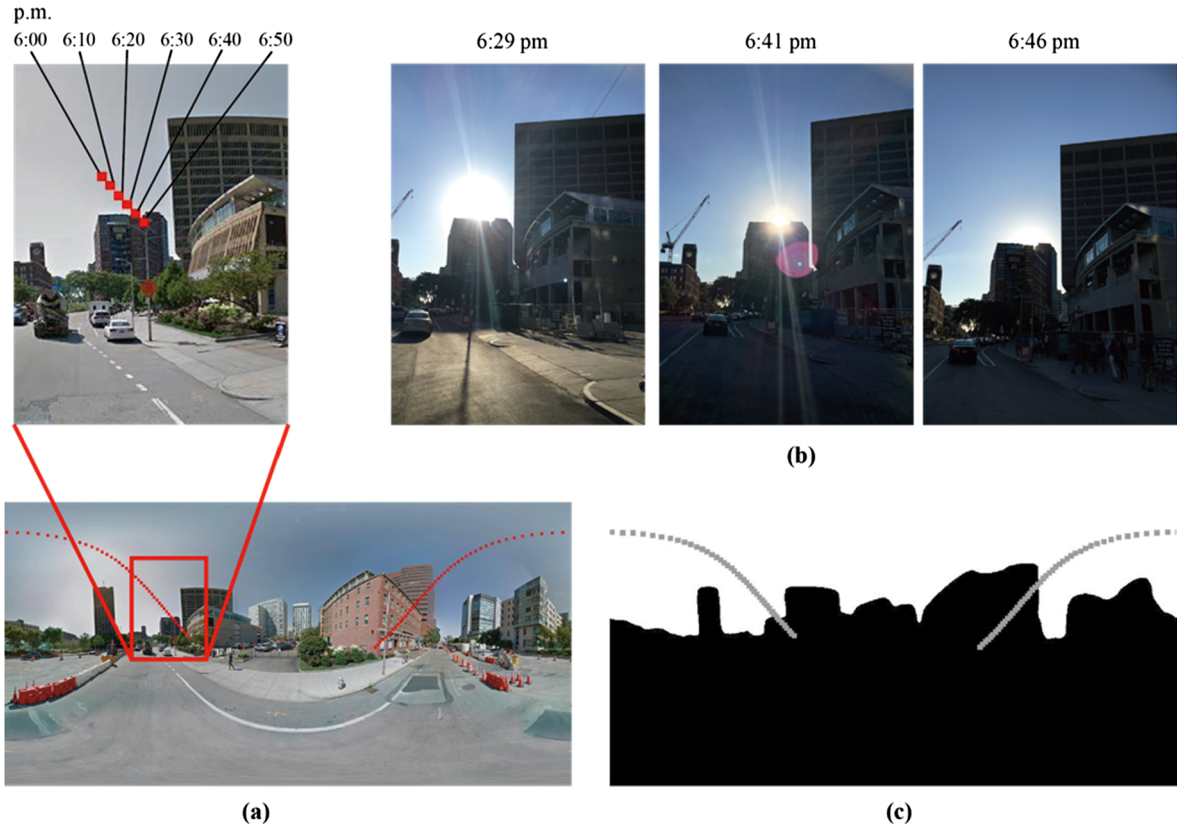


Fig. 9. The comparison of the predicted sun path on a GSV panorama and three photos taken at the same location at three different time points of July 5th, 2018, (a) the sun path of July 5th on a GSV panorama, (b) three photos taken at the same location at different times, (c) the overlay of sun path of July 5th on the segmented GSV panorama, black part represents obstruction pixels and white part represent the sky pixels.

obstructions along the street sides reduces the occurrence and duration of sunrise and sunset sun glares significantly. On June 20th, these streets in the southern Cambridge, especially the Memorial Drive, are exposed to sunrise sun glare more than the rest areas. Those streets in the northwestern and the eastern Cambridge have more potential sunset sun glare occurrence than other regions on June 20th.

4. Discussion

Sun glare is one of the most annoying and dangerous hazards caused by weather for most drivers. It is important for drivers to be informed the potential occurrence of sun glare in order to avoid sun glare caused accidents. Based on the geometrical model of sun position and the locations of drivers, it is possible to predict the occurrence of sun glare by judging the relative angle with the sun from the perspective of drivers. Different from previous studies using digital terrain models to predict the sun glare, this study proposed to use the publicly accessible and globally available Google Street View (GSV) panoramas to predict and map the occurrence of sunrise and sunset sun glares. Considering the fact that GSV images were captured by vehicles on driveways, therefore, the GSV represents what drivers can see on driveways, which make GSV based method more suitable to predict the sun glare. The occurrence of obstruction of sun glare at one location of a specific time can be judged by projecting the sun position to the corresponding GSV panorama and checking whether the sun is located on obstruction or sky pixels in segmented GSV panorama. Therefore, the proposed GSV based method can predict the occurrence of the sun glare more accurately and objectively.

The proposed method was applied in Cambridge, Massachusetts to map the spatio-temporal distributions of sunrise and sunset glares. Results show that the sun glare distributions change significantly in different months of one year. The orientation ranges of streets that potentially have sun glares change monthly because of the changing sun paths in different months. Validation results show that the method can help to predict the sun glare precisely. Theoretically, the method can generate the sun glare occurrence map at day level. In this study, for illustration purpose, we presented the sun glare maps in two days of different months in one year.

The proposed method is totally automatic and without any human intervention. The proposed method provides a simple way to predict the sun glare on driveways at large scales. In addition, the study is based on road networks and the publicly accessible GSV images. Therefore, the method can be applied to any place with GSV service available. This would be very important for those areas with no high spatial resolution spatial data (digital terrain model or building height model) available.

Previous studies have used the digital terrain models to predict the occurrence of the sun glare. However, the digital terrain

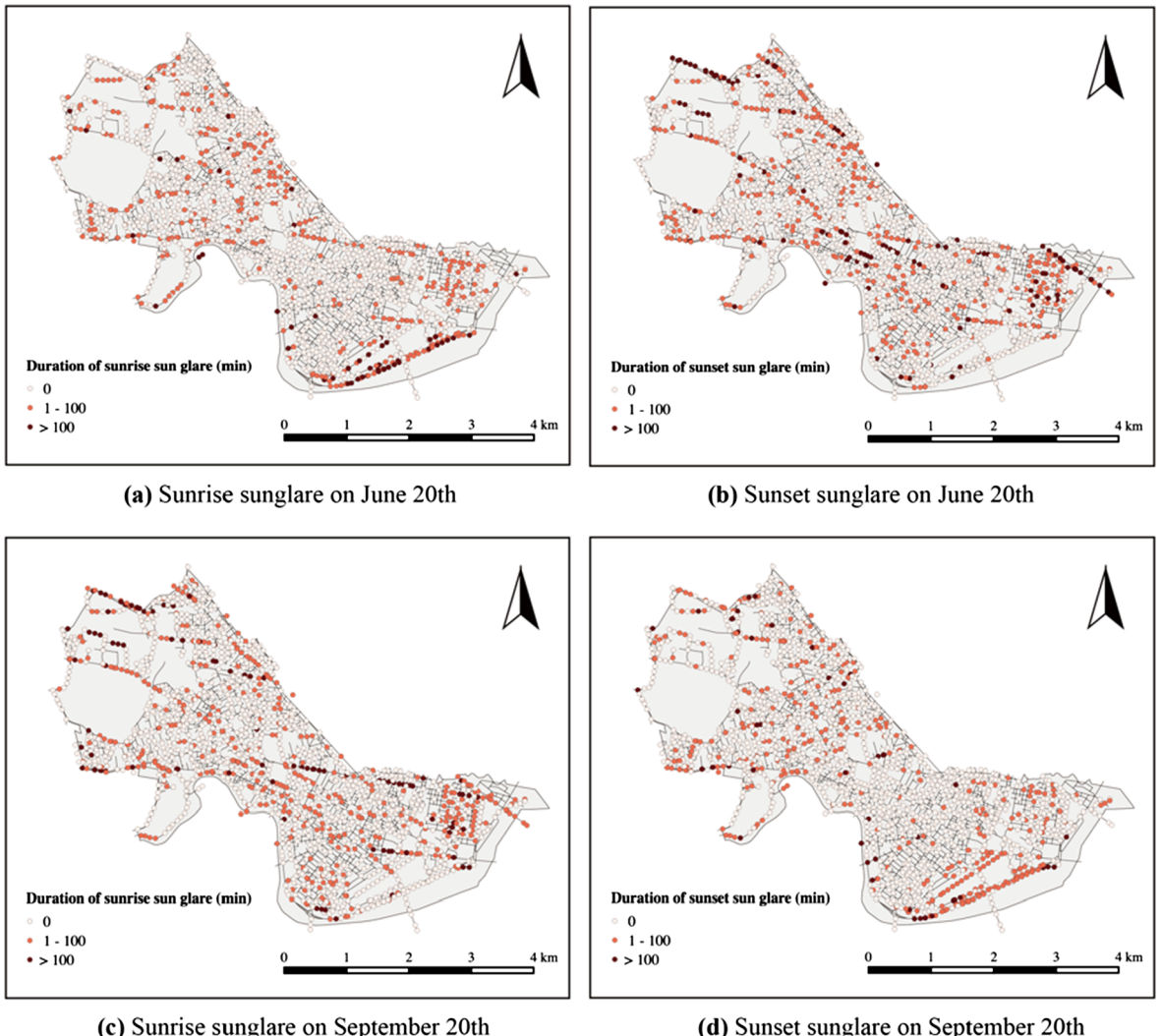


Fig. 10. The spatial distributions of sun glares in Cambridge, MA on June 20th and September 20th, 2018 with consideration of obstructions, (a) the spatial distribution of the sunrise glare on June 20th, (b) the spatial distribution of the sunset glare on June 20th, (c) the spatial distribution of sunrise glare on September 20th, (d) the spatial distribution of actual sunset glare on September 20th.

models usually have very low spatial resolutions, and buildings and trees, which obstruct the sun glares, are usually not considered. Different from the digital terrain model based model, the proposed GSV based method applies the geometrical model of the sun and cars to cylindrical GSV panoramas to predict the obstruction of sun glares at any given time for any given location from driver's perspective. The GSV based method considers the influence of fine-level obstructions on roadsides, such as trees and building blocks.

The proposed method for sun glare prediction would help drivers to be informed about the potential sun glares while driving. On freeways, where nominal speeds and traffic flows are higher, accurate sun glare prediction would help drivers to be prepared and alerted to minimize the negative impacts of sun glare. On urban and suburban roads, where moving cars are sharing the road with pedestrians and cyclists, knowing the occurrence of the sun glare would help to prevent potential crashes caused by sun glare. For navigators and auto insurance companies, the sun glare map can help them to notify the potential sun glare occurrence to drivers, which would help drivers to get a better and safer driving experience. The proposed method for sun glare prediction can also provide useful information for the Department of Transportation. The maintainers of roads can zone those high risky areas and take measures to minimize the potential negative impacts of sun glare on drivers.

There are still some limitations in this study. The seasonal change of the street greenery also influences the occurrence of the sun glare considering the fact that street greenery cannot block the sun glare in leaf-off season. In this study, we only generated the sun glare maps during leaf-on season since the unavailability of GSV images in leaf-off season. Future studies should also generate the sun glare occurrence map for leaf-off season, when the street-level images are available for leaf-off season. Secondly, the atmospheric reflection was not considered in the sun position estimation, which would make the sun position estimation accuracy lower for high latitude areas. Future studies should also consider the atmospheric reflection on the sun position estimation. Currently, the proposed

method only considers the occurrence of the sun glare and the intensity of the sun glare is not considered. Future studies should also consider the intensities of sun glares and the impacts of different sun glare intensities on people of different age-gender groups. In addition, more studies need to be done about how the sun glare influencing the driving experience and the traffic accidents at a large scale.

5. Conclusions

This study proves that it is possible to use Google Street View images to predict and map the occurrence of the sun glare accurately. The proposed method in this study help to generate the spatio-temporal distribution of the occurrence of sun glare, which would help drivers, cyclists, and pedestrians to minimize the negative impacts of sun glare and decrease the potential traffic accidents caused by sun glares. The generated spatio-temporal distribution of sun glare would also help policy makers to redesign road infrastructures to curb the influence of sun glare on drivers, cyclists, and pedestrians. Considering the public accessibility and global availability of street-level images, this study brings a general method to forecast the sun glare for anywhere with street-level images available.

Appendix A. Supplementary material

Supplementary data to this article can be found online at <https://doi.org/10.1016/j.trc.2019.07.013>.

References

- Aune, K., 2017. Sun Glare Detection and Visualization (Master's thesis, NTNU).
- Auffray, B., 2007. Impact of adverse weather on traffic conditions on an American highway, effect of the Sun Glare on Traffic Flow Quality.
- Churchill, A.M., Tripodis, Y., Lovell, D.J., 2012. Sun glare impacts on freeway congestion: geometric model and empirical analysis. *J. Transport. Eng.* 138 (10), 1196–1204.
- Hagita, Mori, 2013. Analysis of the Influence of Sun Glare on Bicycle or Pedestrian Accidents with Turning Vehicle, 13th World Conference on Transport Research.
- Hagita, K., Mori, K., 2014. The effect of sun glare on traffic accidents in Chiba prefecture Japan. *Asian Transport Stud.* 3 (2), 205–219.
- Jurado-Piña, R., Pardillo Mayora, J., 2009b. Methodology to predict driver vision impairment situations caused by sun glare. *Transport. Res. Record: J. Transport. Res. Board* 2120, 12–17.
- Jurado-Pina, R., Pardillo-Mayora, J.M., Jimenez, R., 2010. Methodology to analyze sun-glare-related safety problems at highway tunnel exits. *J. Transport. Eng.* No.6, 545–553.
- Li, X., Zhang, C., Li, W., Ricard, R., Meng, Q., Zhang, W., 2015. Assessing street-level urban greenery using Google Street View and a modified green view index. *Urban Forest. Urban Green.* 14 (3), 675–685.
- Li, X., Ratti, C., Seiferling, I., 2018. Quantifying the shade provision of street trees in urban landscape: a case study in Boston, USA, using Google Street View. *Landscape Urban Plan.* 169, 81–91.
- NOAA, 2014. General Solar Position Calculations. < <http://www.esrl.noaa.gov/gmd/grad/solcalc/solareqns.PDF> > .
- Reda, I., Andreas, A., 2004. Solar position algorithm for solar radiation applications. *Sol. Energy* 76 (5), 577–589.
- Zhou, B., Zhao, H., Puig, X., Fidler, S., Barriuso, A., Torralba, A., 2017, July. Scene parsing through ADE20K dataset. In Proc. CVPR.
- Zhao, H., Shi, J., Qi, X., Wang, X., Jia, J., 2017, July. Pyramid scene parsing network. In: IEEE Conf. on Computer Vision and Pattern Recognition (CVPR), pp. 2881–2890.